

Dark Matter in a bi-metric universe

Carlos Maldonado^{1,*} and Fernando Méndez^{1,†}

¹*Universidad de Santiago de Chile (USACH), Facultad de Ciencia, Departamento de Física, Chile.*

We study the possibility to describe dark matter in a model of the universe with two scale factors and a non-standard Poisson bracket structure characterized by the deformation parameter κ . The dark matter evolution is analyzed in the early stages of the universe, and its relic density is obtained via the Freeze-In and Freeze-Out mechanism. We show that by fixing κ and the initial ratio of energy densities present in the different sectors of the universe, the space of thermal average annihilation cross-sections and dark matter masses compatible with the standard cosmology prior to Big Bang Nucleosynthesis (BBN), is enlarged. This feature of the model is compatible with non-standard cosmology.

I. INTRODUCTION

Dark matter [1–4] and dark energy [5–9] represent about 95% of the total matter-energy content of the universe [10]. Even if it is technically possible to include them in the Einstein equations as a source, the origin of such sources remains unclear until today. In other words, we know they exist and how to incorporate them into the model, but a description in terms of fields – as the remaining 4% of standard model particles – is still unclear.

On the other hand, the standard cosmological model rests on the hypothesis of isotropic and homogeneous three-dimensional space. If there are any inhomogeneities, they [11–17], should be smoothed out during inflation [18, 19]. The metric of the universe, therefore, is described by the Friedmann-Lemaître-Robertson-Walker metric, namely

$$ds^2 = dt^2 + a^2(t) \left(\frac{dr^2}{1 - k r^2} + r^2 d\Omega^2 \right), \quad (1)$$

where $a(t)$ is the scale factor, and r is the radial (dimensionless) coordinate. The constant k is the curvature of spatial sections, which will be taken $k = 0$, according to present measurements [10]. Finally, the present time corresponds to $t = 0$.

A different scenario has been proposed in a series of papers where a universe with two scale factors was considered [20–23]. These scales might represent two causally disconnected patches [24] or two universes in a multi-universe scenario [25]. The main idea of the model is to introduce a sort of interaction through the deformation of the Poisson bracket structure.

The possibility to have a non-canonical Poisson bracket structure and the non-commutative algebras associated [26–30] are the source of a kind of interaction [31–34] whose implications for the dark matter production are investigated in the present paper. Recently, Poisson

bracket deformations have also been studied in the context of closed strings [35, 36] and metaparticles [37], while the implications for cosmology were discussed in [38–41].

In the present approach, we describe the universe by two scale factors a, b , and the Hamiltonian

$$H = \frac{NG}{2} \left[\frac{\pi_a^2}{a} + \frac{1}{G^2} \left(a k_a - \frac{\Lambda_a}{3} a^3 \right) \right] + \frac{NG}{2} \left[\frac{\pi_b^2}{b} + \frac{1}{G^2} \left(b k_b - \frac{\Lambda_b}{3} b^3 \right) \right], \quad (2)$$

$$\equiv H_a + H_b, \quad (3)$$

where π_a, π_b are the conjugate momenta of a and b , respectively ¹. N is an auxiliary field (chosen $N = 1$ at the end of calculations) related to the time invariance reparametrization. The spatial curvatures k_a, k_b will be set to zero. Finally, the Λ_a, Λ_b , are the cosmological constants of each patch.

The Poisson bracket structure that introduces the interaction between the patches is

$$\{a_\alpha, a_\beta\} = 0, \quad \{a_\alpha, \pi_\beta\} = \delta_{\alpha\beta}, \quad \{\pi_\alpha, \pi_\beta\} = \theta \epsilon_{\alpha\beta} \quad (4)$$

with θ a constant parameter and $\{\alpha, \beta\} \in \{a, b\}$. In what follows we will use the dimensionless parameter κ as the deformation parameter, defined as $\theta = \kappa G^{-1}$.

The field equations derived from this Hamiltonian system are first order. They can be recast as the following set of second order equations

$$2a\ddot{a} + \dot{a}^2 = \Lambda_a a^2 - k_a + 2\kappa\dot{b}, \quad (5)$$

$$2b\ddot{b} + \dot{b}^2 = \Lambda_b b^2 - k_b - 2\kappa\dot{a}, \quad (6)$$

along with the first order constraint

$$a\dot{a}^2 + b\dot{b}^2 = \frac{\Lambda_a}{3} a^3 - k_a a + \frac{\Lambda_b}{3} b^3 - k_b b. \quad (7)$$

The physical implications of this model for inflation have been discussed in [20]. Different Poisson bracket deformations, including a non-trivial bracket between scale factors, have been analyzed in [21, 22].

* carlos.maldonados@usach.cl

† fernando.mendez@usach.cl

¹ The canonical dimension of scale factors is +1.

In a recent study [23], the effects of including matter in the model have been considered. To do that, we assumed no interaction between matter evolving on each patch and the matter-energy content described through a barotropic fluid.

The numerical analysis showed a *source-sink* effect, that is, the energy content of one patch *drains* to the other, increasing the energy there. If the process ends before the Big Bang Nucleosynthesis (BBN) epoch ($T_{\text{BBN}} \simeq 4$ GeV), in order not to conflict with astrophysical data [42, 43], the standard cosmology is recovered. This dynamic is described in Figure 1.

The evolution of matter (relativistic in a and non-relativistic in b) is shown as a function of the ratio T/T_0 , with T_0 the present temperature of the universe. The two vertical lines, one at T_{end}/T_0 , and the other at T_{BBN}/T_0 , denote temperatures at which the field in b is no longer effective (all the energy was drained to patch a), and the temperature of BBN, respectively. In this particular case, the total drain happens at the ‘right’ moment of the evolution of patch a .

The dynamics previously described turn out to be consistent with a kind of Non-Standard Cosmology scenario [44–48], in particular with the model where a scalar field is introduced to modify the expansion rate of the universe.

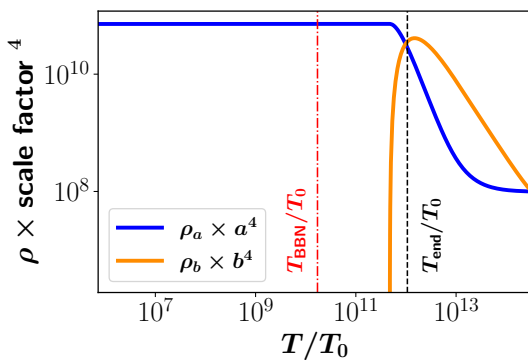


FIG. 1. Energy densities for $\omega = 0$, $\kappa = 10^{-35}$ and $\delta = 1$. The dashed line represents the temperature at which the field on patch b is no longer effective (T_{end}).

In the present research, we extend the study of matter evolution to incorporate dark matter (in one of the patches), considering an approach that is independent of the particle physics model. The paper is organized as follows. In the next section, we provide a brief review of two mechanisms of dark matter (DM) production in the standard model of cosmology. Section III is devoted to the discussion of the relevant equations describing DM in the present model. In section IV we present the numerical results and the analysis of the parameter space consistent with actual observations. The discussion and conclusions are presented in the last section.

II. DARK MATTER IN Λ CDM

The Standard Cosmological Model assumes that DM is established in a radiation domination era. We will focus on two groups of candidates for DM: the Weak Interacting Massive Particles (WIMPs) and Feebly Interacting Massive Particles (FIMPs). The main difference between these two groups is the mechanism of production. WIMPs [49–52] are thermally produced via the Freeze-out mechanism [53], and FIMPs [54–56] are generated in a non-thermal mechanism like the Freeze-in [57–59]. The principal characteristics of these mechanisms will be outlined in what follows, emphasizing the aspects relevant to our proposal.

The number density of DM particles, n_{DM} , satisfies the Boltzmann equation

$$\frac{dn_{\text{DM}}}{dt} + 3H n_{\text{DM}} = -\langle\sigma v\rangle (n_{\text{DM}}^2 - n_{\text{eq}}^2), \quad (8)$$

with $H = \dot{a}/a$ the Hubble parameter, $\langle\sigma v\rangle$ the thermal average annihilation cross-section and n_{eq} is the DM number density of equilibrium.

In the FO mechanism, the DM particles are in thermal equilibrium with the bath of particles in the early universe, and as long as the universe expands, their interactions become inefficient to maintain the thermal equilibrium. Therefore, DM particles leave the thermal bath and freeze their number. This process is referred to as Freeze-Out.

The mechanism is described by eq. (8) and the analytic solution can be obtained in the limit $n_{\text{DM}} \gg n_{\text{eq}}$. In this case, the Yield (Y) of DM – defined as $Y \equiv n_{\text{DM}}/s$, with s the entropy density of the universe – can be estimated as

$$Y \propto \frac{1}{M_{\text{DM}} J(x_{\text{fo}})}, \quad (9)$$

where M_{DM} is the mass of the DM particle, $J(x_{\text{fo}}) = \int_{x_{\text{fo}}}^{\infty} x^{-2} \langle\sigma v\rangle(x) dx$, with x a dimensionless parameter defined by $x = M_{\text{DM}}/T$. The constant x_{fo} is the moment at which the DM particle leaves the thermal bath. Note that for constant thermal average annihilation cross-section, the integral turns out to be $\langle\sigma v\rangle/x_{\text{fo}}$.

Figure 2 shows the Yield of DM in terms of x with $M_{\text{DM}} = 100$ GeV and $\langle\sigma v\rangle = 10^{-11}$ GeV $^{-2}$. The dashed line corresponds to the temperature at which the DM particles decouple from the thermal bath and freeze their number (x_{fo}). The temperature at which BBN epoch start is marked with a dot-dashed line. Finally, the horizontal strip represents the current relic density of DM. The particular set of parameters (M_{DM} and $\langle\sigma v\rangle$) in this figure are excluded in the Λ CDM model due to the fact that they overproduce the current DM relic density.

On the other hand, in the FI mechanism the DM particles are produced in a non-thermal way. They are not in equilibrium with the thermal bath, and therefore, interactions with other particles are feeble and result in that

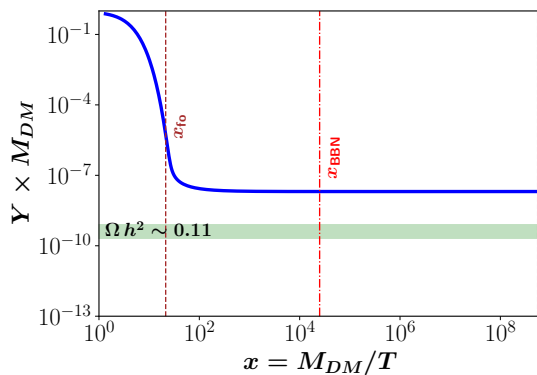


FIG. 2. Yield of Dark Matter particle in Standard Cosmology with mass $M_{DM} = 100$ GeV and thermal average annihilation cross-section $\langle\sigma v\rangle = 10^{-11}$ GeV $^{-2}$ established in the Freeze-Out mechanism.

these particles never thermalize, causing their number to freeze, a process known as Freeze-In.

This scenario is described by Eq.(8) and the analytic solution can be obtained in the limit $n_{eq} \gg n_{DM}$, giving the following estimate of Y

$$Y \propto M_{DM} \langle\sigma v\rangle. \quad (10)$$

That is, the yield is proportional to the thermal average annihilation cross-section, contrasting with the previous case.

The main features of this mechanism are depicted in Figure 3 with $M_{DM} = 100$ GeV and a thermal average annihilation cross-section $\langle\sigma v\rangle = 2 \times 10^{-27}$ GeV $^{-2}$. The dashed line corresponds to the time (temperature) at which these particles freeze their number (x_{fi}) while the horizontal strip is, as before, the current relic density of DM.

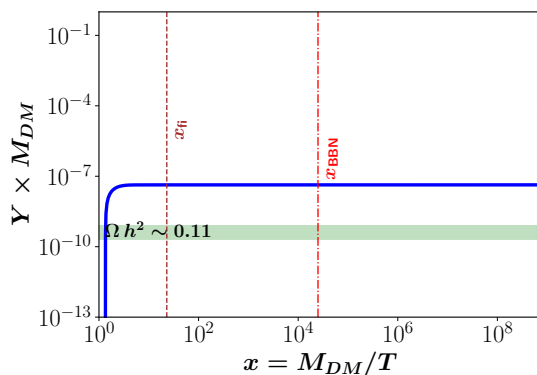


FIG. 3. Yield of Dark Matter particle in Standard Cosmology with mass $M_{DM} = 100$ GeV and thermal average annihilation cross-section $\langle\sigma v\rangle = 2 \times 10^{-27}$ GeV $^{-2}$ established in the Freeze-In mechanism.

Like in the FO case, this set of parameters is excluded because the DM relic is overproduce.

In the following section, we will present the results for both mechanisms in the model with two scale factors described in the previous section.

III. BIMETRIC UNIVERSE WITH MATTER AND DARK MATTER

As anticipated, when the two metrics in presence of matter are considered, the model behaves as a of Non-Standard Cosmology, and the universe expands differently from the standard cosmological scenario. The decaying field in b increases the temperature in the patch a , affecting the production of DM due to the entropy density contribution in the Yield.

The field equations for the case when matter is included have been investigated [23]. No interactions between matter content in a with the matter content in b are assumed. Also, the matter is described as a barotropic fluid in both a and b .

In the present study, we are interested in the case when patch a is filled with relativistic matter, while the barotropic index ω characterizes matter in b . However, for the DM we assume it is present in only one patch, which is understood to be the patch a , for definiteness.

Therefore, the set of equations describing the evolution of matter density in a and b , and DM in a are

$$\dot{\rho}_a + 4 \frac{\dot{a}}{a} \rho_a = 6\kappa M_{Pl}^3 \frac{\dot{a}\dot{b}}{a^3}, \quad (11)$$

$$\dot{\rho}_b + 3(\omega + 1) \frac{\dot{b}}{b} \rho_b = -6\kappa M_{Pl}^3 \frac{\dot{a}\dot{b}}{b^3}, \quad (12)$$

$$\dot{n}_{DM} + 3 \frac{\dot{a}}{a} n_{DM} = -\langle\sigma v\rangle (n_{DM}^2 - n_{eq}^2), \quad (13)$$

with ρ the energy density (and the subscript denoting the patch), M_{Pl} is the reduced Planck mass, κ the deformation parameter and ω the barotropic index of matter in patch b (being $\omega = 1/3$ for relativistic matter in patch a). These equations must consistently solved together with the expressions for the time evolution of the scale factors

$$\dot{a} = a \sqrt{\frac{\rho_a + M_{DM} n_{DM}}{3M_{Pl}^2}}, \quad (14)$$

$$\dot{b} = b \sqrt{\frac{\rho_b}{3M_{Pl}^2}}. \quad (15)$$

Note that $\rho_{DM} = M_{DM} n_{DM}$ in the evolution equation for a . In what follows, the ratio between initial content of matter in b and a will be denoted as δ , that is $\delta = \frac{\rho_b(M_{DM})}{\rho_a(M_{DM})}$ as the most interesting physics occurs at the temperature of DM mass.

In order to investigate this scenario, it is instructive to consider the production mechanisms of FO and FI discussed in the previous section.

For both mechanisms, we use same parameters as those in Figure 2 and 3 which are excluded in the Λ CDM, but are allowed in the present model.

We set the deformation parameter $\kappa = 10^{-35}$, with non-relativistic matter in the patch b ($\omega=0$) and a symmetric initial condition $\delta = 1$. The evolution of Yield can be observed in Figure 4 giving us the current relic density with DM parameters that were discarded in the Λ CDM model.

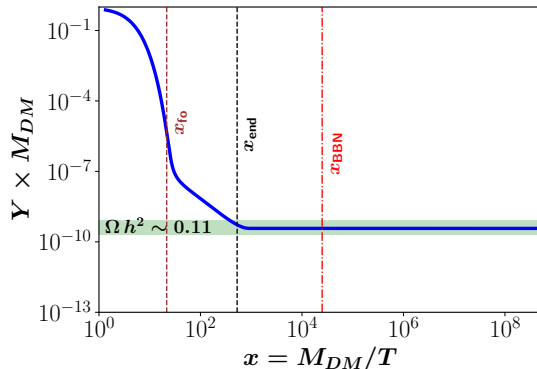


FIG. 4. Yield of Dark Matter particles with mass $M_{DM} = 100$ GeV and thermal average annihilation cross-section $\langle\sigma v\rangle = 10^{-11}$ GeV $^{-2}$ established in the Freeze-Out mechanism in a bimetric universe with $\omega = 0$ in b patch, $\kappa = 10^{-35}$ and $\delta = 1$.

Note also that there are two lines which do not depend on the model. The first one corresponds to the temperature at which DM freezes its number (dotted line x_{fo}), and the second is the BBN temperature (dot-dashed line x_{BBN}). The line x_{end} , corresponds to the moment at which the matter in b is no longer effective and, therefore, the Yield of DM establishes as a constant number. Finally, observe that a condition $x_{end} \leq x_{BBN}$ is required to be consistent with current cosmological data.

For the FI mechanism, we set mass and thermal average annihilation cross-section as done in Figure 3. The deformation parameter is chosen as before, $\kappa = 10^{-35}$, and also the matter fluid in b is non-relativistic ($\omega = 0$) with a symmetric initial condition $\delta = 1$. The evolution of the Yield is depicted in Figure 5.

We can observe the same behavior described above. The time at which the DM freezes its number is the same as the Standard Case, but in this model, the Yield of DM decreases due to the decay of the field in b , giving us the current relic density of DM.

It is important to mention that the quantity x_{end} depends only on the value of κ and δ , i.e., for the same value of κ and δ , the time at which the effect of field b is no longer effective is the same.

Then, it is natural to ask if the values of parameters ($\langle\sigma v\rangle$, M_{DM} , κ , δ , ω) shown before are the only possibility consistent with the current DM relic density.

A fast answer is shown in Figure 6. A parameter space plot for FO mechanism where, the horizontal axis is the DM mass parameter M_{DM} , and the vertical axis contains the values of thermal average annihilation cross section $\langle\sigma v\rangle$. Parameters κ and δ are fixed $\kappa = 10^{-35}$ and $\delta = 1$.

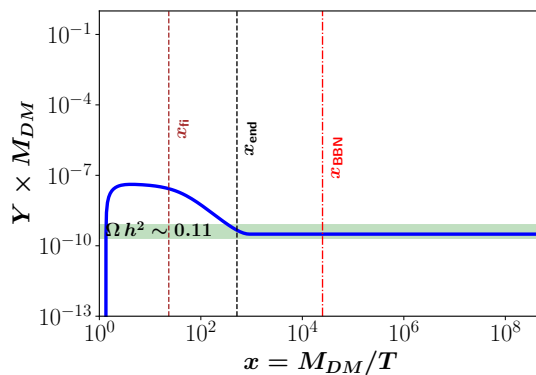


FIG. 5. Yield of Dark Matter particles with mass $M_{DM} = 100$ GeV and thermal average annihilation cross-section $\langle\sigma v\rangle = 2 \times 10^{-27}$ GeV $^{-2}$ established in the Freeze-In mechanism in a bimetric universe with $\omega = 0$ in b patch, $\kappa = 10^{-35}$ and $\delta = 1$.

The continuous line corresponds to the DM mass and thermal average annihilation cross-section, consistent with DM relic density observations.

Finally, the region for which the matter content of b decays after BBN time (temperature) is shown as the region $T_{end} < T_{BBN}$. We call this *the forbidden zone*.

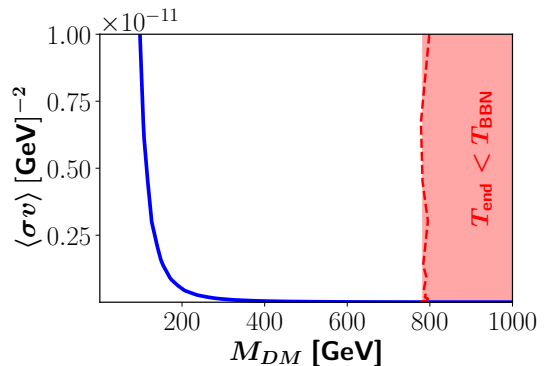


FIG. 6. Space of parameter in thermal average annihilation cross-section and mass of the Dark Matter particle which gives the current Yield in the Freeze-Out mechanism for $\omega = 0$ in b patch, $\kappa = 10^{-35}$ and $\delta = 1$. The red area corresponds to temperatures below the Big Bang Nucleosynthesis and therefore are forbidden to ensure the correct measurements of the Λ CDM model.

Results for the FI mechanism are shown in Figure 7. The forbidden zone is the same as before since it depends on κ and δ only. The continuous line shows the DM mass and thermal average annihilation cross-sections giving the current values of Yield.

Previous results can be extended for different values of the deformation parameter κ , initial condition δ , and for different content of matter in patch b ($\omega \neq 0$).

The numerical results of the study of those scenarios are the central topic of the next section.

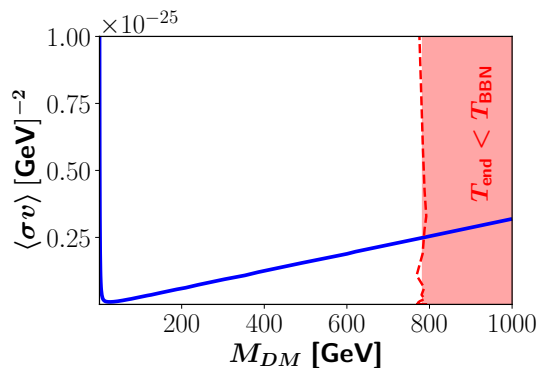


FIG. 7. Space of parameter in the thermal average annihilation cross-section and mass of the Dark Matter particle which gives the current Yield in the Freeze-In mechanism for $\omega = 0$ in b patch, $\kappa = 10^{-35}$ and $\delta = 1$. The red area corresponds to temperatures below the Big Bang Nucleosynthesis and therefore are forbidden to ensure the correct measurements of the Λ CDM model.

IV. PARAMETER SPACE

When DM is not present, the values of κ compatible with present observations are those for which the drain of energy from b to a finish before BBN epoch (see [46]). When DM is considered, non-zero values of κ also affect the production of DM relic density.

In order to investigate these effects, in the following subsections we consider two cases. In the first, the matter content of the b sector is non-relativistic ($\omega = 0$), and in the second, we consider b patch filled with relativistic matter ($\omega = 1/3$).

For both, we consider the FO and FI mechanisms and also will address the problem of non-symmetric initial configuration.

A. Non-relativistic matter in b patch ($\omega = 0$)

For the FO mechanism and $\delta = 1$, the space of allowed DM mass and thermal average annihilation cross-section for different values of κ , are the solid lines shown in Figure 8. The dashed lines (with corresponding colors) show the boundary of the forbidden zone so that for all points to the right of this boundary, T_{end} are below of the BBN temperature.

Large values of DM mass with smaller values of thermal average annihilation cross-section are allowed as κ increases.

Now we consider fixed $\kappa = 10^{-35}$ for variable initial condition δ in the FO mechanism. The Figure 9 shows a similar behavior to the one just described. Dashed lines show the boundary of the forbidden regions (one for each value of δ) and we see that for less symmetric conditions, it is possible to consider higher values of DM mass and smaller values of the thermal average annihilation cross-

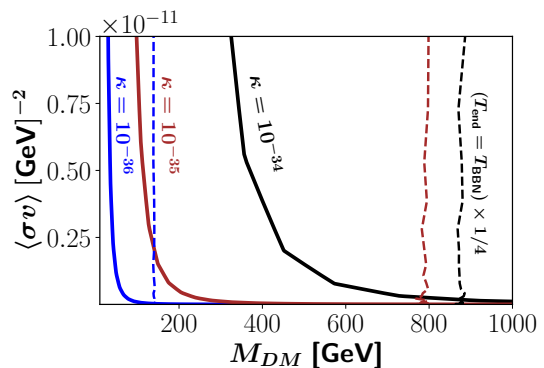


FIG. 8. Space of parameter in the thermal average annihilation cross-section and mass of the Dark Matter particle which gives the current Yield in the Freeze-Out mechanism for different values of κ , $\omega = 0$ and $\delta = 1$. The dashed lines correspond to $T_{\text{end}} = T_{\text{BBN}}$. Points to the right of this line will be in conflict with actual measurements of the Λ CDM model. The black dashed line is shifted by a factor of 1/4.

sections.

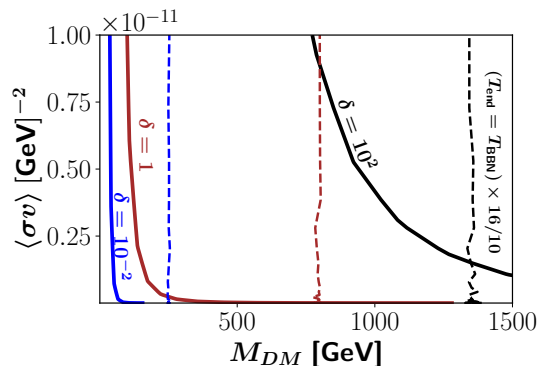


FIG. 9. Space of parameter in the thermal average annihilation cross-section and mass of the Dark Matter particle which gives the current Yield in the Freeze-Out mechanism for different values of δ , $\omega = 0$ and $\kappa = 10^{-35}$. The dashed lines correspond to $T_{\text{end}} = T_{\text{BBN}}$. Points to the right of this line will be in conflict with actual measurements of the Λ CDM model. The black dashed line is shifted by a factor of 16/10.

For the FI mechanism, we have also explored the cases of varying κ with symmetric initial conditions and the opposite one, namely, fixed κ and variable initial conditions. The Figure 10, exhibits the allowed parameter space (solid lines) for different values of κ , and $\delta = 1$.

An appealing feature of the model is the existence of two values of DM mass for the same value of the thermal average annihilation cross-section, at least for $\kappa < 10^{-35}$. For $\kappa \rightarrow 0$, the graph shows a tendency to collapse the solid line, indicating that the two values of DM mass should differ by a small amount. This characteristic deserves a careful analysis exceeding the scope of the present work, but to be reported in the near future.

For the case of variable initial conditions and fixed κ ,

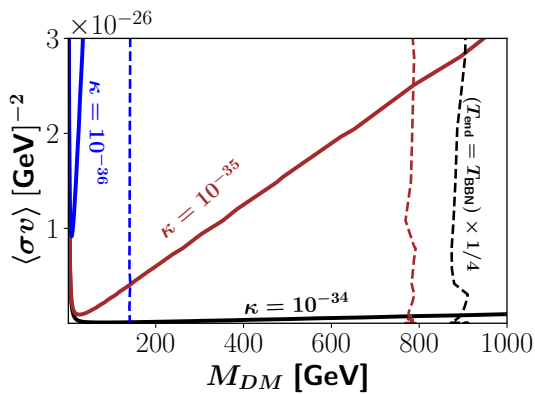


FIG. 10. Space of parameter in the thermal average annihilation cross-section and mass of the Dark Matter particle which gives the current Yield in the Freeze-In mechanism for different values of κ , $\omega = 0$ and $\delta = 1$. The dashed lines correspond to $T_{\text{end}} = T_{\text{BBN}}$. Points to the right of this line will be in conflict with actual measurements of the Λ CDM model. The black dashed line is shifted by a factor of 1/4.

results are shown in Figure 11 with $\kappa = 10^{-35}$. The inside panel shows a zoom for small values of DM mass ($M_{DM} < 100$ GeV). As before, higher values in δ give us branches that open in a wide angle.

Finally note that for the FO mechanism, the allowed parameters (solid lines) with higher values of δ behaves like allowed parameters for higher values of κ . Instead, for the FI mechanism, the higher values of δ mimic the behavior of smaller values of κ .

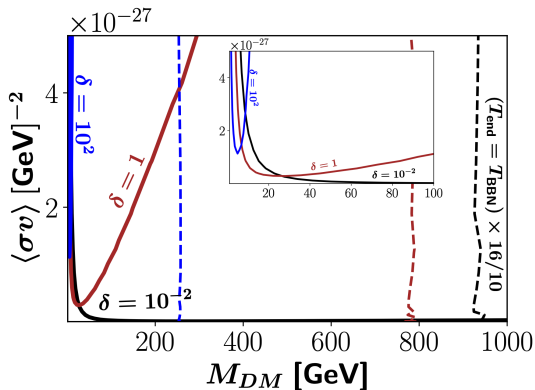


FIG. 11. Space of parameter in the thermal average annihilation cross-section and mass of the Dark Matter particle which gives the current Yield in the Freeze-In mechanism for different values of δ , $\omega = 0$ and $\kappa = 10^{-35}$. The dashed lines correspond to $T_{\text{end}} = T_{\text{BBN}}$. Points to the right of this line will be in conflict with actual measurements of the Λ CDM model. The black dashed line is shifted by a factor of 16/10.

B. Relativistic matter in b patch ($\omega = 1/3$)

When we consider a relativistic fluid in b patch ($\omega = 1/3$) in the FO mechanism, the possible values of κ and δ giving the current DM relic density, turn out to be more restricted.

However, no solution was found for κ with $\delta < 10^2$, so that the current DM relic density is reproduced prior to BBN, in the Freeze-Out mechanism.

The Figure 12 shows different values of κ for $\delta = 10^3$. The boundaries of the forbidden zones are shifted to higher values of DM mass. Also, we observe that for large values of DM mass, all curves (solid ones) go to a fixed value of the thermal average annihilation cross-section. However, we emphasize that only the masses to the left of the vertical lines (the boundaries of forbidden zones) give the correct amount of the current DM relic density and, at the same time, $T_{\text{end}} > T_{\text{BBN}}$.

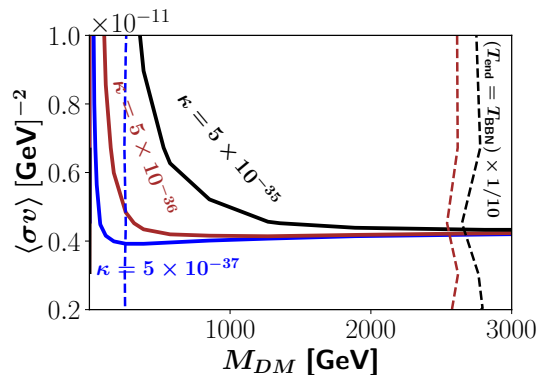


FIG. 12. Space of parameter in the thermal average annihilation cross-section and mass of the Dark Matter particle which gives the current Yield in the Freeze-Out mechanism for different values of κ , $\omega = 1/3$ and $\delta = 10^3$. The dashed lines correspond to $T_{\text{end}} = T_{\text{BBN}}$. Points to the right of this line will be in conflict with actual measurements of the Λ CDM model. The black dashed line is shifted by a factor of 1/10.

The Figure 13 shows the parameter space for a constant value of $\kappa = 5 \times 10^{-35}$ and different values of δ . In contrast with the situation depicted in Figure 9 ($\omega = 0$), in this case there is a shift of the curves in the y-axis for higher values of δ .

For the FI mechanism the behavior is different from the case of $\omega = 0$, but close to the FO case with $\omega = 0$. Therefore, this mechanism allows $\delta < 10^2$, in contrast with previous one. In Figure 14 we set $\delta = 1$ while κ changes, but only two cases have been considered. High values of κ shift the curves down in the y-axis, allowing small values of the thermal average annihilation cross-section with high masses of DM. The appearance of a minimum is no longer valid.

In the case of a constant value of the deformation parameter ($\kappa = 10^{-35}$) and varying δ , the allowed parameters are shown in Figure 15. As before, no considerable differences can be observed for the two values of δ showed.

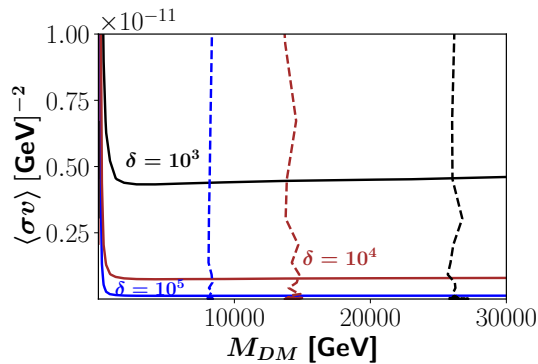


FIG. 13. Space of parameter in the thermal average annihilation cross-section and mass of the Dark Matter particle which gives the current Yield in the Freeze-Out mechanism for different values of δ , $\omega = 1/3$ and $\kappa = 5 \times 10^{-35}$. The dashed lines correspond to $T_{\text{end}} = T_{\text{BBN}}$. Points to the right of this line will be in conflict with actual measurements of the Λ CDM model.

The forbidden zone is shifted to the left for higher δ , as expected.

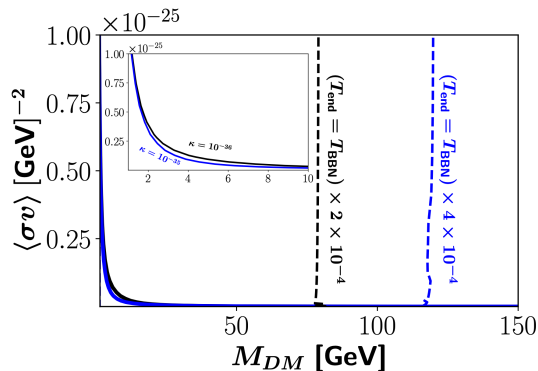


FIG. 14. Space of parameter in the thermal average annihilation cross-section and mass of the Dark Matter particle which gives the current Yield in the Freeze-In mechanism for different values of κ , $\omega = 1/3$ and $\delta = 1$. The dashed lines correspond to $T_{\text{end}} = T_{\text{BBN}}$. Points to the right of this line will be in conflict with actual measurements of the Λ CDM model.

V. DISCUSSION AND CONCLUSIONS

In this study we have presented the evolution of DM density in a model of the universe described by two scale factors when there is a non-standard Poisson bracket structure imposed. In a recent study, the evolution of matter in such a model has been considered and it was shown that the system evolves as a type of non-standard cosmology.

When DM is added to one of the patches it is natural to ask if the evolution of DM is affected due to the evolution

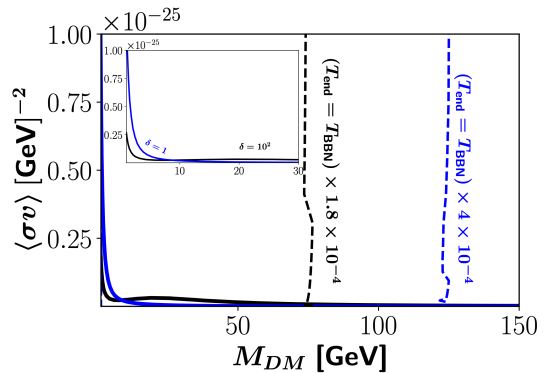


FIG. 15. Space of parameter in the thermal average annihilation cross-section and mass of the Dark Matter particle which gives the current Yield in the Freeze-In mechanism for different values of δ , $\omega = 1/3$ and $\kappa = 10^{-35}$. The dashed lines correspond to $T_{\text{end}} = T_{\text{BBN}}$. Points to the right of this line will be in conflict with actual measurements of the Λ CDM model.

of matter in the other patch present in the model.

We have shown, by using numerical calculations, that the evolution of DM is indeed affected, but different values of the parameters of the model render such evolution consistent with actual measurement of DM relics.

In order to do that, two groups of DM candidates were considered: WIMPs and FIMPs, which are related with the mechanism of production Freeze-out (FO) and Freeze-in (FI), respectively. We studied the scenario in which DM and relativistic matter coexists in one patch, with the second patch containing either relativistic or non-relativistic matter.

For the case when patch b contains non-relativistic matter, we showed that the FO mechanism for a symmetric initial condition (the same amount of energy in both patches at the beginning of the evolution), higher values of the deformation parameter κ allow higher DM masses as the thermal average annihilation cross-section diminishes. A similar behavior is observed for a constant κ , but with initial conditions highly asymmetric ($\delta = 10^2$, and higher).

For the FI mechanism, under the same conditions, we observe that there is also a set of DM masses and thermal average annihilation cross-sections compatible with the observed actual DM relic. However, in this case, the allowed values of $\langle\sigma v\rangle$ and M_{DM} have a minimum, either for variable κ and symmetric initial conditions or, for a fixed κ and asymmetric initial conditions.

The case for which the b -patch is filled with relativistic matter, the possibility of considering values of thermal average annihilation cross-sections and DM masses different from the usual ones, is also present. Compared to the previous case (non-relativistic matter in b), here it is possible to reach larger values of DM masses.

For the FO mechanism, it was not possible to find a symmetric initial condition compatible with different values of κ in order to obtain the actual DM relic density

prior to BBN.

The FI mechanism, instead, shows a peculiar behavior. Apart from the fact that the symmetric initial condition is admissible, curves with different κ (and fixed δ), or fixed κ (and variable δ), are very close, that is, the range of DM masses and thermal average annihilation cross-sections do not significantly change under variations (independent) of κ and δ .

Let us finish our analysis emphasizing the main result: it is possible to consider DM production in this model in such a way that the DM relic obtained via FI or FO mechanisms is compatible with the actual observations. The space of parameters of thermal average annihilation cross-sections and DM masses is enlarged, admitting values which are ruled out in the standard cosmology.

As a final comment, let us point out that in non-standard cosmologies, a similar situation is verified due to the fact that the *source-sink* effect is implemented by a $\Gamma \rho_\phi$ term, where Γ is the decay rate of a new field (ϕ) present in the early universe. This Γ can be re-

lated to the temperature at which the field must decay (T_{end}). Indeed, by choosing $M_{DM} = 100$ GeV, $\langle\sigma v\rangle = 10^{-11}$ GeV $^{-2}$ and $T_{\text{end}} = 0.1$ GeV, the DM relic density in a FO mechanism is reproduced [47] with the same parameter shown in our analysis but from a completely different perspective. In the case of the FI mechanism choosing $M_{DM} = 100$ GeV, $\langle\sigma v\rangle = 10^{-22}$ GeV $^{-2}$ and $T_{\text{end}} = 500$ GeV reproduce the DM relic density [46], but in our model such a thermal average annihilation cross-section does not reproduce the correct value of DM prior to BBN. This is interesting because for the same values of DM mass it is possible to reach lower values of cross-sections.

VI. ACKNOWLEDGEMENTS

This work was supported by Dicyt-USACH grants USA1956-Dicyt (CM) and Dicyt-041931MF (FM).

-
- [1] F. Zwicky, *Helv. Phys. Acta* **6**, 110 (1933).
 - [2] K. C. Freeman, *Astrophys. J.* **160**, 811 (1970).
 - [3] G. Bertone and D. Hooper, *Rev. Mod. Phys.* **90**, 045002 (2018), arXiv:1605.04909 [astro-ph.CO].
 - [4] P. Salucci, *Found Phys.* **48**, 1517 (2018), arXiv:1807.08541 [astro-ph.CO].
 - [5] A. G. Riess, A. V. Filippenko, P. Challis, A. Clocchiatti, A. Diercks, P. M. Garnavich, R. L. Gilliland, C. J. Hogan, S. Jha, R. P. Kirshner, and et al., *The Astronomical Journal* **116**, 1009–1038 (1998).
 - [6] S. Perlmutter, G. Aldering, G. Goldhaber, R. A. Knop, P. Nugent, P. G. Castro, S. Deustua, S. Fabbro, A. Goobar, D. E. Groom, and et al., *The Astrophysical Journal* **517**, 565–586 (1999).
 - [7] P. J. E. Peebles and B. Ratra, *Rev. Mod. Phys.* **75**, 559 (2003), arXiv:astro-ph/0207347.
 - [8] M. Li, X.-D. Li, S. Wang, and Y. Wang, *Commun. Theor. Phys.* **56**, 525 (2011), arXiv:1103.5870 [astro-ph.CO].
 - [9] K. Bamba, S. Capozziello, S. Nojiri, and S. D. Odintsov, *Astrophys. Space Sci.* **342**, 155 (2012), arXiv:1205.3421 [gr-qc].
 - [10] P. A. Zyla *et al.* (Particle Data Group), *PTEP* **2020**, 083C01 (2020).
 - [11] P. Sikivie, *Phys. Rev. Lett.* **48**, 1156 (1982).
 - [12] A. Vilenkin, *Physics Report* **121**, 263 (1985).
 - [13] A. Lukas, B. A. Ovrut, K. S. Stelle, and D. Waldram, *Phys. Rev. D* **59**, 086001 (1998), arXiv:arXiv:hep-th/9803235 [hep-th].
 - [14] R. Durrer, *New Astron. Rev.* **43**, 111 (1999).
 - [15] E. Flanagan, S.-H. Tye, and I. Wasserman, *Phys. Rev. D* **62**, 024011 (2000), arXiv:hep-ph/9909373 [hep-ph].
 - [16] J. W. Moffat, *JCAP* **05**, 001 (2006), arXiv:astro-ph/0505326.
 - [17] K. Bolejko, M.-N. Celerier, and A. Krasinski, *Class. Quant. Grav.* **28**, 164002 (2011), arXiv:1102.1449 [astro-ph.CO].
 - [18] P. Peebles and A. Vilenkin, *Phys. Rev. D* **59**, 063505 (1999), arXiv:hep-ph/9811375 [hep-ph].
 - [19] A. D. Linde, *Particle physics and inflationary cosmology*, Vol. 5 (Harwood Academic Publishers, 1990) arXiv:hep-th/0503203.
 - [20] H. Falomir, J. Gamboa, F. Méndez, and P. Gondolo, *Phys. Rev. D* **96**, 083534 (2017), arXiv:1707.04670 [gr-qc].
 - [21] H. Falomir, J. Gamboa, P. Gondolo, and F. Méndez, *Phys. Lett. B* **785**, 399 (2018), arXiv:1801.07575 [hep-th].
 - [22] H. Falomir, J. Gamboa, and F. Mendez, *Symmetry* **12**, 435 (2020).
 - [23] C. Maldonado and F. Mendez, *Phys. Rev. D* **103**, 123505 (2021), arXiv:2103.11235 [gr-qc].
 - [24] S. Rasouli, J. Marto, and P. Moniz, *Physics of the Dark Universe* **24**, 100269 (2019).
 - [25] A. Linde, *Rept. Prog. Phys.* **80**, 022001 (2017), arXiv:1512.01203 [hep-th].
 - [26] F. Bayen, M. Flato, C. Fronsdal, A. Lichnerowicz, and D. Sternheimer, *Annals Phys.* **111**, 61 (1978).
 - [27] B. V. Fedosov, *Journal of Differential Geometry* **40**, 213 (1994).
 - [28] M. de Wilde and P. B. A. Lecomte, *Letters in Mathematical Physics* **7**, 487 (1983).
 - [29] M. Kontsevich, *Lett. Math. Phys.* **66**, 157 (2003), arXiv:q-alg/9709040.
 - [30] A. S. Cattaneo and D. Indelicato, *Lond. Math. Soc. Lect. Note Ser.* **323**, 79 (2004), arXiv:math/0403135.
 - [31] V. P. Nair and A. P. Polychronakos, *Phys. Lett. B* **505**, 267 (2001), arXiv:hep-th/0011172.
 - [32] J. Gamboa, M. Loewe, F. Mendez, and J. C. Rojas, *Mod. Phys. Lett. A* **16**, 2075 (2001), arXiv:hep-th/0104224.
 - [33] C. Acatrinei, *JHEP* **09**, 007 (2001), arXiv:hep-th/0107078.
 - [34] D. Karabali, V. P. Nair, and A. P. Polychronakos, *Nucl. Phys. B* **627**, 565 (2002), arXiv:hep-th/0111249.

- [35] L. Freidel, R. G. Leigh, and D. Minic, *Phys. Rev. D* **96**, 066003 (2017), arXiv:1707.00312 [hep-th].
- [36] L. Freidel, R. G. Leigh, and D. Minic, *JHEP* **09**, 060 (2017), arXiv:1706.03305 [hep-th].
- [37] L. Freidel, J. Kowalski-Glikman, R. G. Leigh, and D. Minic, *Phys. Rev. D* **99**, 066011 (2019), arXiv:1812.10821 [hep-th].
- [38] P. Berglund, T. Hübsch, and D. Minić, *Phys. Lett. B* **798**, 134950 (2019), arXiv:1905.08269 [hep-th].
- [39] P. Berglund, T. Hübsch, and D. Minic, *Int. J. Mod. Phys. D* **28**, 1944018 (2019), arXiv:1905.09463 [gr-qc].
- [40] P. Berglund, T. Hübsch, and D. Minic, *LHEP* **2021**, 186 (2021), arXiv:2010.15610 [hep-th].
- [41] L. Freidel, J. Kowalski-Glikman, R. G. Leigh, and D. Minic, (2021), arXiv:2104.00802 [gr-qc].
- [42] D. J. H. Chung, E. W. Kolb, and A. Riotto, *Phys. Rev. D* **60**, 063504 (1999), arXiv:hep-ph/9809453 [hep-ph].
- [43] E. W. Kolb, A. Notari, and A. Riotto, *Phys. Rev. D* **68**, 123505 (2003), arXiv:hep-ph/0307241 [hep-ph].
- [44] G. F. Giudice, E. W. Kolb, and A. Riotto, *Phys. Rev. D* **64**, 023508 (2001), arXiv:hep-ph/0005123 [hep-ph].
- [45] L. Visinelli, *Symmetry* **10**, 11 (2018), arXiv:1710.11006 [astro-ph.CO].
- [46] C. Maldonado and J. Unwin, *JCAP* **06**, 37 (2019), arXiv:1902.10746 [hep-ph].
- [47] P. Arias, N. Bernal, A. Herrera, and C. Maldonado, *JCAP* **10**, 47 (2019), arXiv:1906.04183 [hep-ph].
- [48] N. Bernal, F. Elahi, C. Maldonado, and J. Unwin, *JCAP* **11**, 26 (2019), arXiv:1909.07992 [hep-ph].
- [49] G. Bertone, D. Hooper, and J. Silk, *Phys. Rept.* **405**, 279 (2005), arXiv:hep-ph/0404175 [hep-ph].
- [50] G. Arcadi, M. Dutra, P. Ghosh, M. Lindner, Y. Mambrini, M. Pierre, S. Profumo, and F. S. Queiroz, *Eur. Phys. J.* **C78**, 203 (2018), arXiv:1703.07364 [hep-ph].
- [51] T. Lin, *Proceedings, Theoretical Advanced Study Institute in Elementary Particle Physics: Theory in an Era of Data (TASI 2018): Boulder, Colorado, USA, June 4-29, 2018*, *PoS* **333**, 009 (2019), arXiv:1904.07915 [hep-ph].
- [52] D. Hooper, *Proceedings, Theoretical Advanced Study Institute in Elementary Particle Physics: Theory in an Era of Data (TASI 2018): Boulder, Colorado, USA, June 4-29, 2018*, *PoS TASI2018*, 010 (2019), arXiv:1812.02029 [hep-ph].
- [53] E. W. Kolb and M. S. Turner, *The Early Universe*, Vol. 69 (CRC Press, 1990).
- [54] L. J. Hall, K. Jedamzik, J. March-Russell, and S. M. West, *JHEP* **1003**, 080 (2010), arXiv:0911.1120 [hep-ph].
- [55] X. Chu, T. Hambye, and M. H. G. Tytgat, *JCAP* **1205**, 034 (2012), arXiv:1112.0493 [hep-ph].
- [56] N. Bernal, M. Heikinheimo, T. Tenkanen, K. Tuominen, and V. Vaskonen, *International Journal of Modern Physics A* **32** (2017), 10.1142/S0217751X1730023X, arXiv:hep-ph/1706.07442.
- [57] J. McDonald, *Phys.Rev.Lett.* **88**, 091304 (2002), arXiv:hep-ph/0106249 [hep-ph].
- [58] K.-Y. Choi and L. Roszkowski, *Proceedings on 11th International Symposium on Particles, Strings and Cosmology (PASCOS 2005): Gyeongju, Korea, 30 May - 4 June 2005*, *AIP Conf. Proc.* **805**, 30 (2006), [30(2005)], arXiv:hep-ph/0511003 [hep-ph].
- [59] A. Kusenko, *Phys. Rev. Lett.* **97**, 241301 (2006), arXiv:hep-ph/0609081 [hep-ph].